THE ASTROPHYSICAL JOURNAL, 315:L135–L139, 1987

HIGH-VELOCITY EMISSION IN YOUNG SUPERNOVA REMNANTS: SN 1006 AND SN 1572

ROBERT P. KIRSHNER[1,2]
Harvard-Smithsonian Center for Astrophysics
P. FRANK WINKLER[1]
Department of Physics, Middlebury College; and Institute of Astronomy, University of Cambridge
AND
ROGER A. CHEVALIER[2]
Department of Astronomy, University of Virginia
Received 1986 December 26; accepted 1987 February 6

ABSTRACT

We have detected broad Hα emission from the SN 1006 remnant with a FWHM velocity of 2600 ± 100 km s^{-1}. This emission is similar to that seen in the remnant of SN 1572 (Tycho's SNR), which we have also observed with 4 times the previous spectral resolution and measured a FWHM for Hα of 1800 km s^{-1}. In both cases, the ratio of broad to narrow Hα line emission and the measured width of the broad line are in reasonable accord with the nonradiative shock model. Using the nonradiative model to interpret the line widths, we compare the derived shock velocity with proper motion measurements to derive distances of 1.4–2.1 kpc to SN 1006 and 2.0–2.8 kpc to SN 1572. The range of distances depends on whether electrons are thermalized behind the shock along with the ions. These distance measures are useful in deriving the physical properties of young supernova remnants: the circumstantial evidence is strong that SN 1006 is expanding into a substantially lower density medium than SN 1572. The distances may also prove useful in calibrating the extragalactic distance scale through Type Ia supernovae, but uncertainties in interpreting the historical record remain an obstacle.

Subject headings: nebulae: supernova remnants — shock waves

I. INTRODUCTION

The 2000 km s^{-1} broad wings on the Hα line in the remnant of SN 1572 (Tycho's supernova remnant) have been interpreted as emission from a nonradiative shock (Chevalier, Kirshner, and Raymond 1980, hereafter CKR; Chevalier and Raymond 1978; McKee and Hollenbach 1980). This mechanism accounts for both the narrow and broad components of the hydrogen emission and the absence of lines from other atoms by considering the effect of a fast shock on neutral hydrogen. In this picture, narrow Balmer-line emission results from direct collisional excitation of hydrogen atoms by fast electrons and protons, and the broad component arises from charge exchange that produces a fast-moving excited hydrogen atom.

Supernova remnants in which the Balmer lines are very strong compared to the usual forbidden lines that characterize SNRs (Fesen, Blair, and Kirshner 1985) include the remnant of SN 1572 (Kirshner and Chevalier 1978), the optical remnant of SN 1006 (Schweizer and Lasker 1978), and four SNRs in the LMC (Tuohy *et al.* 1982). In SN 1006, the faint, wispy filaments discovered by van den Bergh (1976) show pure Balmer emission, but Lasker (1981) searched without success for the broad component predicted by the nonradiative shock model.

In this *Letter* we report the discovery of the broad component predicted by CKR and sought by Lasker, and we use the nonradiative shock model to derive the kinematic properties of the remnant. As shown by CKR, the width of the broad line provides a measure of the shock velocity, and the ratio of the flux in the broad component to that in the narrow Hα emission provides a second independent estimate of the shock velocity. In this *Letter* we also report observations of the Hα emission from SN 1572 at 4 times the spectral resolution used by CKR and interpret the results in the nonradiative model.

II. OBSERVATIONS

a) SN 1006

We observed SN 1006 with the CTIO 4 m telescope, Ritchey-Chrétien spectrograph, and the No. 3 GEC CCD on the night of 1986 March 3/4. A 600 line mm^{-1} grating (No. 420) and a long slit of width 1″.64 were used to give a dispersion of 1.57 Å $pixel^{-1}$ and an effective resolution of 3.9 Å (FWHM). The slit was oriented at P.A. 72° and positioned to cross the brightest filaments along the NW rim of SN 1006 at a small angle. The slit position is illustrated in Figure 1 (Plate L1); approximate coordinates for the slit center are RA: $14^h59^m03^s$, decl.: −41°33′13″ (1950).

[1] Visiting Astronomer, Cerro Tololo Interamerican Observatory.
[2] Visiting Astronomer, Kitt Peak National Observatory, National Optical Astronomy Observatories, operated by AURA, Inc. under contract with the National Science Foundation.

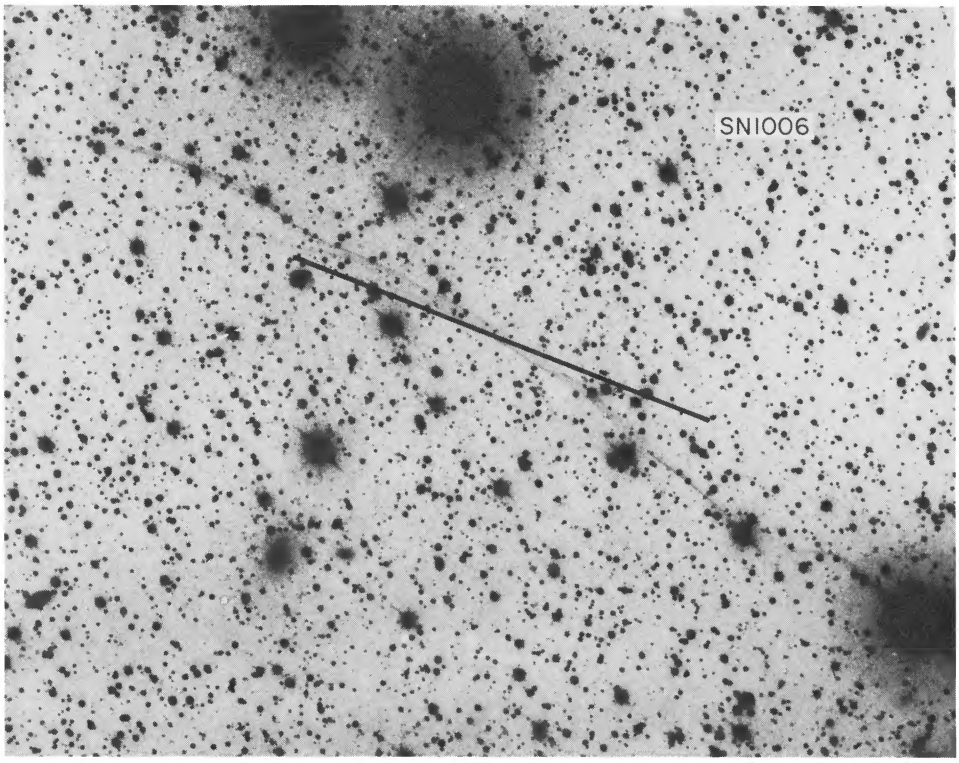

FIG. 1

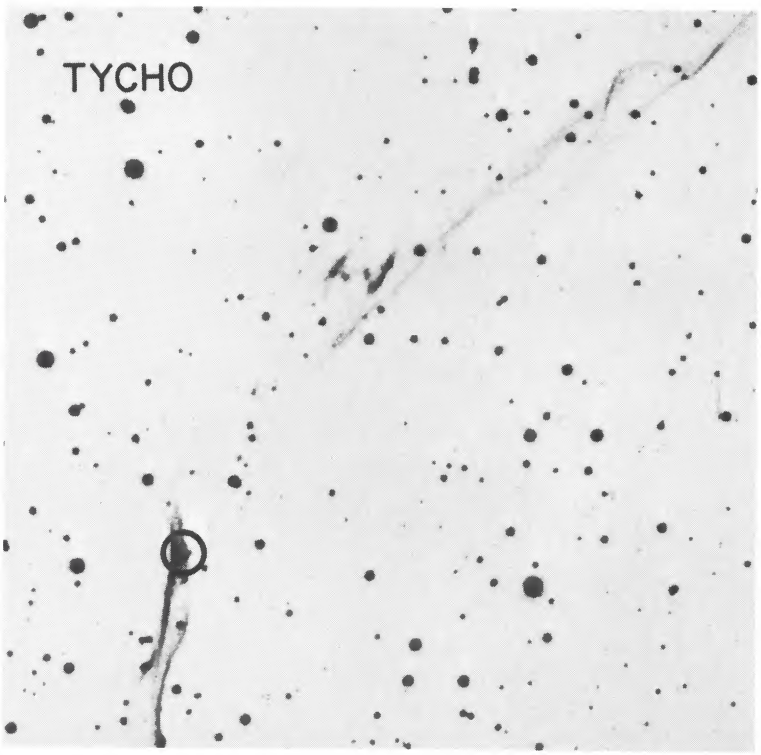

FIG. 3

FIG. 1.—Slit position for long-slit observations of SN 1006
FIG. 3.—Location of IIDS aperture on the eastern rim of SN 1572. The image is a CCD frame in Hα obtained at KPNO with the Prime Focus CCD.

KIRSHNER, WINKLER, AND CHEVALIER (*see* pages L135 and L136)

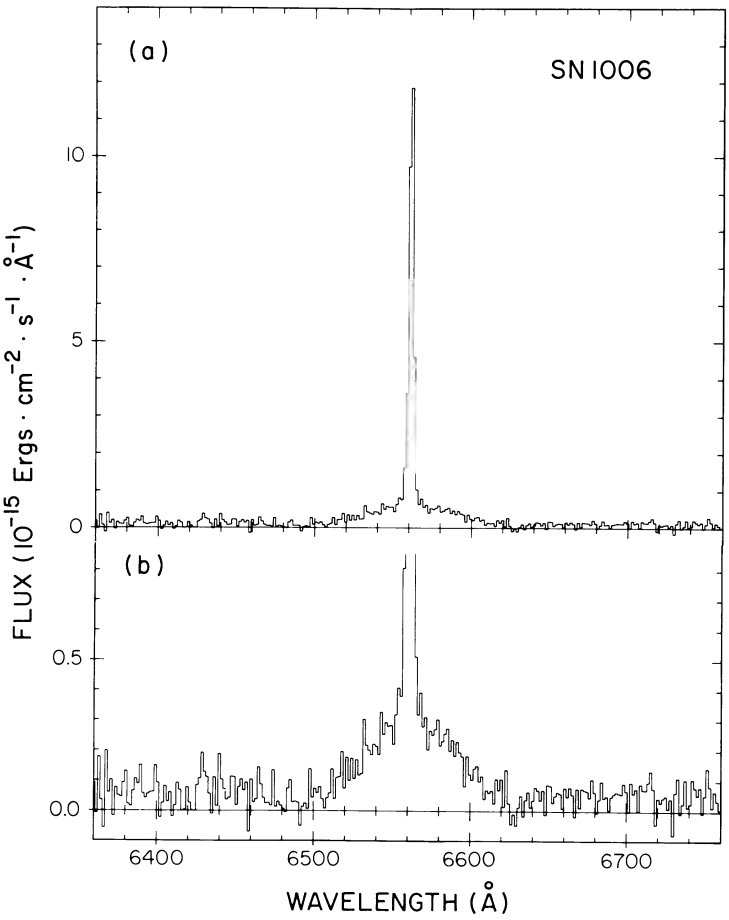

FIG. 2.—The Hα line of SN 1006. Fig. 2*a* illustrates the strength of the narrow component relative to the broad, while Fig. 2*b* shows the width of the broad component.

A total integration time of 10,800 s was accumulated in six contiguous 1800 s integrations. The data have been combined, sky-subtracted using regions at the ends of the slit, and reduced to fluxes using the IRAF long-slit reduction routines. Broad wings on the Hα line are apparent in the two-dimensional spectrum even before sky subtraction. We have summed the data over 19″ along the slit, including the brightest portion of the filament, to give the spectrum shown in Figure 2.

The Hα line clearly has two components: an unresolved component and broad wings of width 57 Å (FWHM) equivalent to a velocity of 2600 $\pm$ 100 km s^{-1}. Spectra of comparison lamps and of other SNRs observed on the same night with the same set-up show only narrow line profiles: there can be no doubt that the wings observed in SN 1006 are real. The relative intensity in the broad and narrow components is $I_b/I_n = 0.77 \pm 0.08$, and the average surface brightness in Hα, summing both components, is approximately 1×10^{-5} ergs cm^{-2} s^{-1} sr^{-1}.

Following the prediction of CKR, Lasker (1981) searched unsuccessfully for the broad component of Hα at a position 5′ NE of ours. He measured a surface brightness in unresolved Hα about 2/3 the value we have observed and placed an upper limit on the broad component. Our positive detection of broad Hα wings is at about the level of Lasker's upper limit and is due principally to the excellent throughput of the CCD spectrometer on the CTIO 4 m.

No lines other than Hα were detected in the 6150–7050 Å band covered by our spectra to a level of 5% of the narrow Hα flux.

b) SN 1572

The SN 1572 observations were carried out at KPNO using the Mayall 4 m and the IIDS attached to the RC spectrograph on 1979 September 17/18. The entrance aperture was a 3.″2 circle; when used with the 831 lines/mm^{-1} grating, this gave an effective resolution of 5.6 Å, 4 times better than that used by CKR. The aperture was centered on the knot labeled "g" by Kamper and van den Bergh (1978), taking into account its considerable proper motion. The nominal position in 1979 September was RA: $00^h23^m05^s.1$, decl.: +63° 52′ 40″ (1950), and is illustrated in Figure 3 (Plate L1). The IIDS is a dual beam image dissector, with simultaneous sky measurement through a second aperture 52″ E or W. The total integration time was 6400 s. The spectra in each beam were sky-subtracted, summed, and fluxed using the standard KPNO programs.

As shown in Figure 4, we used an isolated line (6610 Å) from our comparison spectrum as a template for the un-

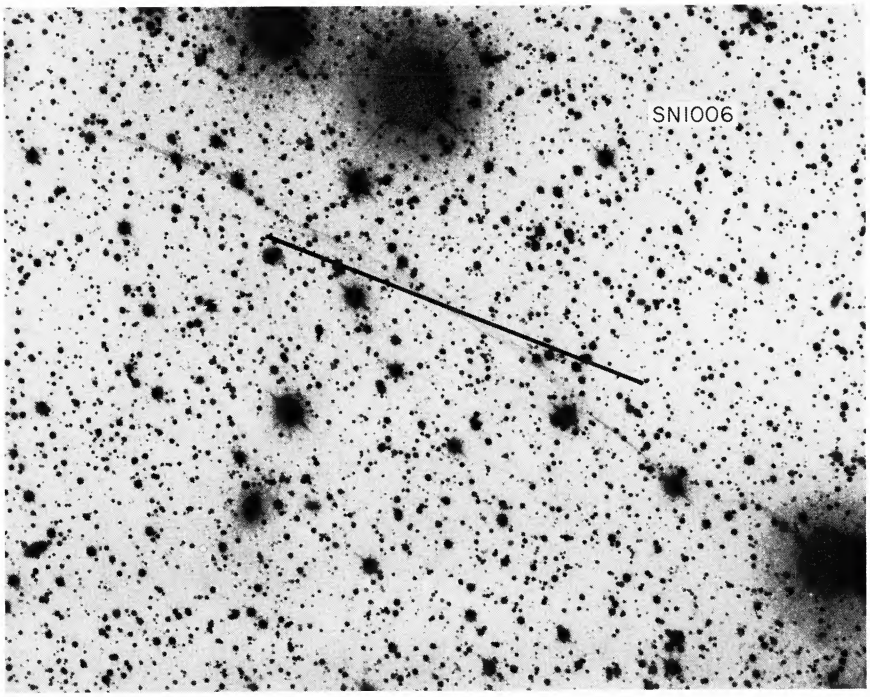

FIG. 1

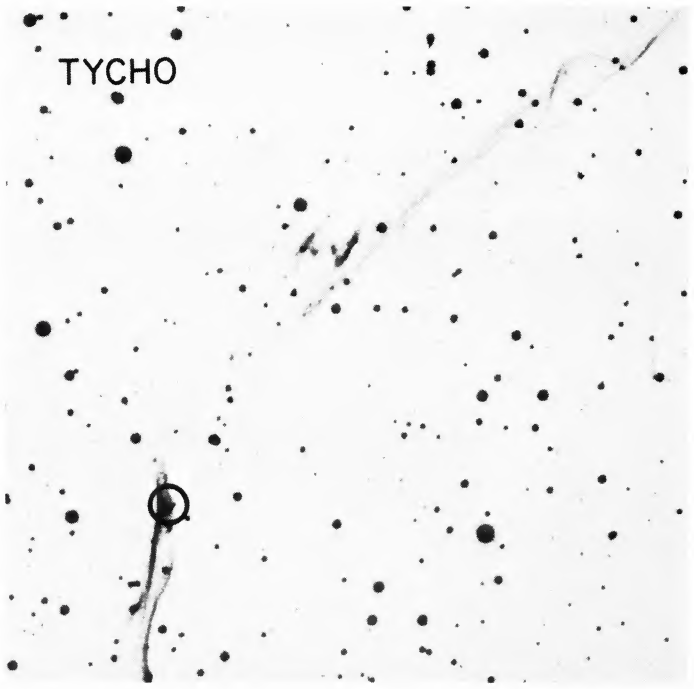

FIG. 3

FIG. 1.—Slit position for long-slit observations of SN 1006
FIG. 3.—Location of IIDS aperture on the eastern rim of SN 1572. The image is a CCD frame in Hα obtained at KPNO with the Prime Focus CCD.

KIRSHNER, WINKLER, AND CHEVALIER (*see* pages L135 and L136)

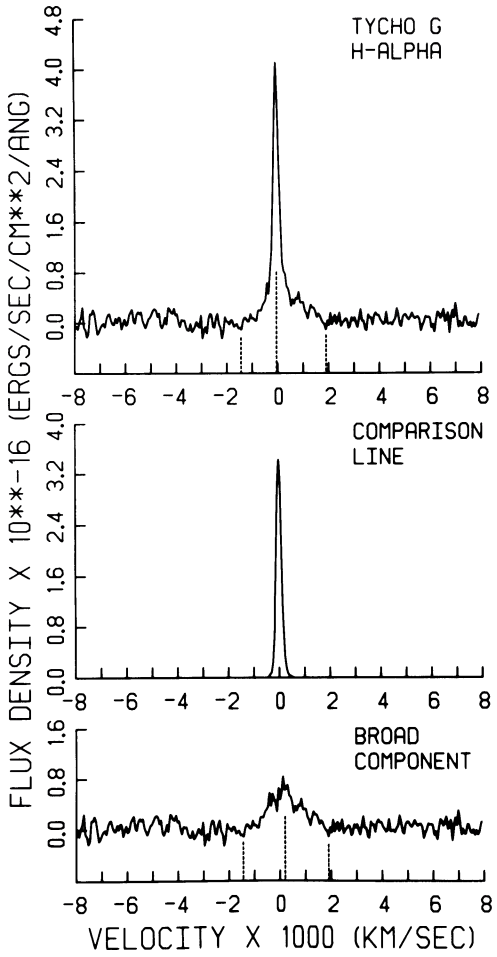

FIG. 4.—The Hα line of SN 1572. (*a*) The observations. (*b*) A comparison line profile observed with the identical instrument. (*c*) The observations with a suitably scaled instrumental profile subtracted. Note the small asymmetry in the line profile.

resolved component. The comparison line was shifted and scaled, and then subtracted from the observations to leave the spectrum of the broad component. We find the ratio of the broad to narrow flux is $I_b/I_n = 1.08 \pm 0.16$. This is consistent with the CKR value of 0.4–1.3, but much more precise. The FWHM of the broad component is 1800 ± 100 km s^{-1}. Again, this is consistent with the much cruder measure of CKR who found 2300 ± 500 km s^{-1}. The observed surface brightness of the combined narrow and broad components is 2×10^{-5} ergs cm^{-2} s^{-1} sr^{-1}. No other line as strong as 5% of the narrow Hα was detected in the interval 6400–7000 Å covered by our spectra. Finally, we note a small asymmetry in the broad component. Its center is shifted to the red of the narrow component by 5.2 ± 0.4 Å, corresponding to a velocity of $+238$ km s^{-1}.

III. INTERPRETATION

The pure Balmer-line spectrum of remnants such as Tycho's and SN 1006 has been explained by the nonradiative shock models of Chevalier and Raymond (1978; see also McKee and Hollenbach 1980). In this model, the SNR shock wave propagates into an ambient interstellar medium that is partially neutral. Neutral atoms are not greatly affected by the shock and drift into the hot postshock region where they can be collisionally excited to produce narrow Balmer-line emission at near zero velocity. Some of the slow neutral atoms will undergo charge exchange with hot shocked ions to produce a population of fast neutral atoms that is responsible for the broad lines. This model has been applied to observations in the Cygnus Loop (Kirshner and Taylor 1976; Raymond *et al.* 1983) as well as to SN 1572, SN 1006, and the Magellanic Cloud remnants.

In the model, the width of the broad Balmer lines is a measure of the postshock thermal velocity distribution, modified by the velocity width of the charge-exchange cross section. The observed widths of 2600 km s^{-1} for SN 1006 and 1800 km s^{-1} for SN 1572 correspond to values of 2100 km s^{-1} and 1450 km s^{-1} for v_0, the bulk velocity of the shocked gas in CKR's model A, in which only protons are thermalized behind the shock. For a fully ionized plasma with 10% He by number, and thermalization of electrons as well as ions (CKR model B), the corresponding v_0 values are 2900 km s^{-1} for SN 1006 and 2000 km s^{-1} for SN 1572. In either case, the shock velocity v_s is $4/3\ v_0$.

The relative intensity of the broad and narrow components gives an independent measure of v_0, because the charge-exchange and excitation cross sections are functions of velocity. Using equation (5) and Figure 2 of CKR, we have constructed Figure 5, which gives the expected ratio of broad to narrow flux as a function of v_0 for model A. As the figure indicates, the v_0 for SN 1006 is nominally in the range 1875 ± 75 km s^{-1}, and for SN 1572, it lies in the range 1675 ± 100 km s^{-1}.

The agreement between the interpretation of the line widths and the line strengths in this model, where only the protons are thermalized, is satisfactory. CKR do not present an explicit calculation of the broad to narrow ratio for model B, although it would generally require a larger value of v_0 than model A, since the protons would have a smaller share of the energy. The fact that theory does not instruct us clearly on the properties of the equilibration behind the shock remains an uncertainty in applying this model.

The width of the line is a more direct measure of the shock velocity than the ratio of the narrow to broad components because a calculation of that ratio requires a substantial correction for the relative effects of the Lyman lines in populating levels for the two components. As a result, we adopt the range of velocities for models A and B for SN 1006 and for SN 1572 to give values of v_s of 2800–3870 km s^{-1} for SN 1006 and 1930–2670 km s^{-1} for SN 1572. The uncertainties are dominated by unknown factors in the interpretation, rather than by measuring uncertainties.

Proper motions for SN 1006 were measured by Hesser and van den Bergh (1981) to be $0''.39 \pm 0''.6$ yr^{-1}. We assume that the observed proper motion refers to the shock velocity as it propagates into a neutral cloud. Then the implied distance to SN 1006 is 1.5–2.1 kpc. The baseline for the proper motion measurements was only 5 yr; twice that time span is now available, and the measurement is worth repeating to higher precision.

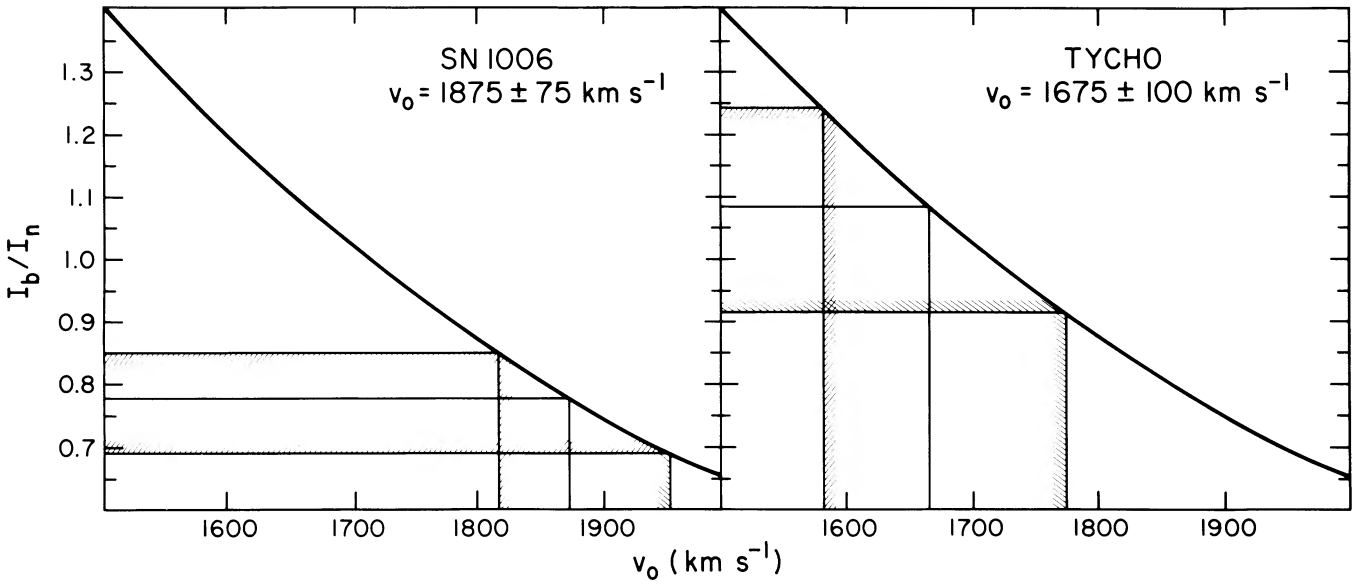

FIG. 5.—The observed range of broad to narrow line strengths interpreted through the model A of CKR to yield a range of postshock velocities for both SN 1006 and SN 1572.

Similarly, the measured proper motion for knot "g" in SN 1572 is 0".20 ± 0".01 yr^{-1} (Kamper and van den Bergh 1978). This corresponds to a distance of 2.0–2.8 kpc, in reasonable accord with recent estimates based on H I absorption by Albinson *et al.* (1986) who find $2.2^{+1.5}_{-0.6}$ kpc. This is also consistent with the result of Black and Raymond (1984) who show that interstellar absorption lines in stars toward SN 1572 imply that the 21 cm data do not exclude distances as small as 2 kpc. Recently, de Vaucouleurs (1985) has summarized the problem of the distance to SN 1572 and concluded that 3.2 ± 0.3 kpc is a good estimate.

The inclination of the shock to the line of sight is a significant geometrical factor which is not well accounted for in the simplest analysis. Some limit on that inclination comes from the asymmetry of the broad Hα observed in SN 1572. There, the shift of about 240 km s^{-1} compared to the inferred shock velocity of (4/3) (2000 km s^{-1}) or 2667 km s^{-1} implies an angle of order 6° between the shock front and the line of sight. This implies that the observed surface brightness of the shock is about 10 times the face-on value. Taking into account the reddening to SN 1572, and using the emissivity calculated by Chevalier and Raymond (1978), we find that the implied preshock density of neutral hydrogen is 0.3 cm^{-3}. Because this estimate only accounts for the neutral hydrogen, it is a lower limit to the total preshock density. This value is in moderately good accord with the density of 0.9 inferred by CKR based on interpretation of the X-ray surface brightness.

The same computation for SN 1006, allowing for zero reddening and a surface brightness that is down by a factor of 2, yields a density of the surround that is 16 times smaller than for SN 1572. Other lines of evidence also converge on a smaller surrounding density for SN 1006. Assuming the same explosion energy and an adiabatic blast wave, the ambient density scales as age^{-3} × velocity^{-5}. For SN 1006, with a larger age and a larger velocity than SN 1572, a smaller density seems indicated.

A low density for the medium surrounding SN 1006 is made plausible by its relatively high galactic latitude of 14°.5, which corresponds to a distance of more than 400 pc from the Galactic plane at the distances indicated by this analysis. For comparison, SN 1572 is only 1°.4 from the plane, corresponding to a height of 60 pc at the distance required by our shock velocity and the proper motion. The X-ray spectra for SN 1006 and for SN 1572 differ sharply: while SN 1572 shows strong X-ray lines, SN 1006 does not. Hamilton, Sarazin, and Szymkowiak (1986*a*, *b*) attribute that contrast to differences in ionization due to a lower density surrounding SN 1006, which is consistent with the picture developed here.

IV. SUPERNOVAE AND THE EXTRAGALACTIC DISTANCE SCALE

If we take these distances seriously, then the absolute magnitude of SN 1572 and of SN 1006 can be estimated. Following the assumptions of CKR for the apparent magnitude at maximum ($m_v = -4.4$), color at maximum ($B - V = 0.15$), and absorption to SN 1572 ($A_v = 2.1$), we find that a distance of 2.4 kpc, in the middle of our range, gives $M_B = -19.1$ with an uncertainty from the distance estimate of ±0.4 mag. De Vaucouleurs uses a somewhat different set of assumptions to infer $M_V = -18.55$, corresponding to $M_B = -18.7$. For SN 1006, the historical record is more challenging to interpret, with estimates of the apparent visual magnitude at maximum ranging from −6 (Pskovskii 1978) to −9.5 (Stephenson, Clark, and Crawford 1977). If we follow Stephenson, Clark, and Crawford, the inferred $M_B = -20.5$, with no contribution for reddening. If we follow Pskovskii, a substantial reddening correction inferred from the color at maximum light makes $M_B = -17.9$.

These values are in reasonable accord with extragalactic values for Type Ia supernovae (Branch and Bettis 1978; Sandage and Tammann 1982). The error in the distance due

to uncertainties in the interpretation of our spectra only amounts to ± 0.4 mag. While the photometric uncertainty compounded with the error in the reddening estimates make this a perilous way to calibrate the Hubble constant, the historical evidence is consistent with the possibility that these two supernovae were of Type Ia. However, as noted by Doggett and Branch (1985), the photometric evidence alone can never be conclusive.

We note that Sandage and Tammann (1985) prefer $M_B = -19.74$ for SN Ia, while the analysis of de Vaucouleurs (1985) implies $M_B = -18.7$. The estimates for SN 1006 and SN 1572 given here, where the mean M_B lies between -18.5 and -19.8 depending on which value is used for SN 1006, cannot decide this issue. Even so, to reduce the uncertainty in the distance to the two supernovae cannot make the overall uncertainty in the extragalactic scale larger.

Some uncertainties remain in the astrophysics of this method of shock excitation, and improved measurements of the proper motions are certainly possible, but those uncertainties seem unlikely to be as large as a factor of 2. Larger errors more likely lurk within the estimates of the apparent magnitude and reddening than with the distance. Of course, if SN 1572 and SN 1006 were not identical to the events that we now classify spectroscopically as SN Ia, then the comparison is not valid and no inference about the extragalactic distance scale is permitted. While no spectra of these objects near maximum light will be forthcoming, a deeper understanding of the remnants that we see today, coupled with study of the corresponding extragalactic objects, may yet shed some light on this problem.

This work was supported in part by the National Science Foundation through grants AST83-09496 and AST84-42225 to the University of Michigan, AST85-16537 to Harvard University, AST85-20557 and NASA grant NAG-8389 to Middlebury College, and AST84-13138 to the University of Virginia. P. F. W. acknowledges the kind hospitality of the Institute of Astronomy, University of Cambridge, where much of this work was performed. We are grateful to John Raymond and to A. J. S. Hamilton for their thoughtful comments and to Sidney van den Bergh for providing the image of SN 1006. The IRAF is distributed by the National Optical Astronomy Observatories, which is operated by the Association of Universities for Research in Astronomy, Inc. under contract to the National Science Foundation.

REFERENCES

Albinson, J. S., Tuffs, R. J., Swinbank, E., and Gull, S. F. 1986, *M.N.R.A.S.*, **219**, 427.
Black, J. H., and Raymond, J. C. 1984, *A.J.*, **89**, 411.
Branch, D., and Bettis, C. 1978, *A.J.*, **83**, 224.
Chevalier, R. A., Kirshner, R. P., and Raymond, J. C. 1980, *Ap. J.*, **235**, 186 (CKR).
Chevalier, R. A., and Raymond, J. C. 1978, *Ap. J. (Letters)*, **225**, L27.
de Vaucouleurs, G. 1985, *Ap. J.*, **289**, 5.
Doggett, J. B., and Branch, D. 1985, *A.J.*, **90**, 2303.
Fesen, R. A., Blair, W. P., and Kirshner, R. P. 1985, *Ap. J.*, **292**, 29.
Hamilton, A. J. S., Sarazin, C. L., and Szymkowiak, A. E. 1986*a*, *Ap. J.*, **300**, 698.
_____. 1986*b*, *Ap. J.*, **300**, 713.
Hesser, J. E., and van den Bergh, S. 1981, *Ap. J.*, **251**, 549.
Kamper, K., and van den Bergh, S. 1978, *Ap. J.*, **224**, 851.
Kirshner, R. P., and Chevalier, R. A. 1978, *Astr. Ap.*, **67**, 267.
Kirshner, R. P., and Taylor, K. 1976, *Ap. J. (Letters)*, **208**, L83.
Lasker, B. M. 1981, *Ap. J.*, **244**, 517.
McKee, C. F., and Hollenbach, D. J. 1980, *Ann. Rev. Astr. Ap.*, **18**, 219.
Pskovskii, Yu. P. 1978, *Soviet Astr.–AJ*, **22**, 420.
Raymond, J. C., Blair, W. P., Fesen, R. A., and Gull, T. R. 1983, *Ap. J.*, **275**, 636.
Sandage, A. R., and Tammann, G. A. 1982, *Ap. J.*, **256**, 339.
_____. 1985, in *Supernovae as Distance Indicators*, ed. N. Bartel (Berlin: Springer-Verlag), p. 1.
Schweizer, F., and Lasker, B. M. 1978, *Ap. J.*, **226**, 167.
Stephenson, F. R., Clark, D. H., and Crawford, D. F. 1977, *M.N.R.A.S.*, **180**, 567.
Tuohy, I. R., Dopita, M. A., Mathewson, D. S., Long, K. S., and Helfand, D. J. 1982, *Ap. J.*, **261**, 473.
van den Bergh, S. 1976, *Ap. J. (Letters)*, **208**, L17.

ROGER A. CHEVALIER: Leander McCormick Observatory, University of Virginia, P. O. Box 3818, University Station, Charlottesville, VA 22903-0818

ROBERT P. KIRSHNER: Center for Astrophysics MS-19, 60 Garden Street, Cambridge, MA 02138

P. FRANK WINKLER: Department of Physics, Middlebury College, Middlebury, VT 05753

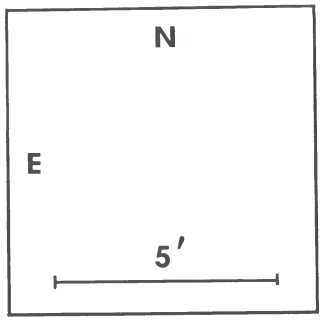

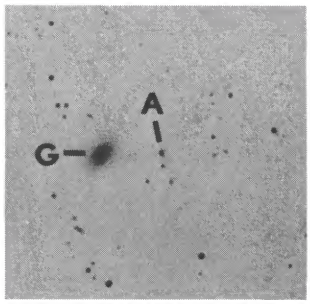

1229.3+6430

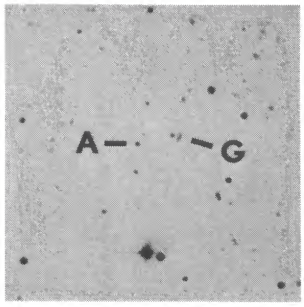

0200.9−0858

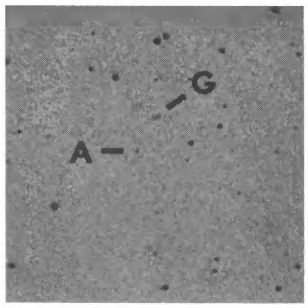

0226.8−1041

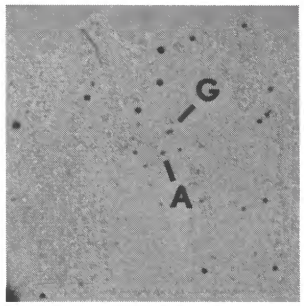

0317.9−1949

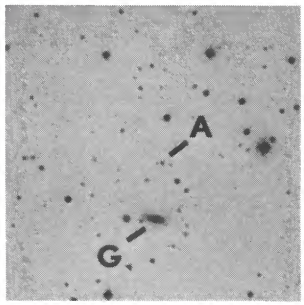

0745.1+5545

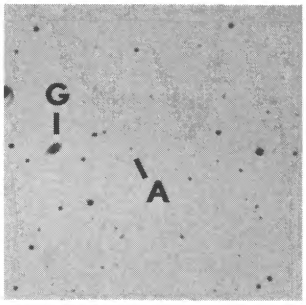

0950.2+0804

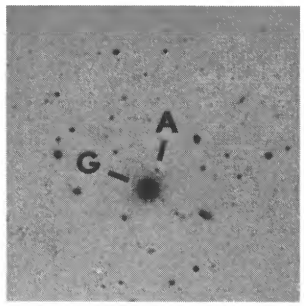

1109.3+3544

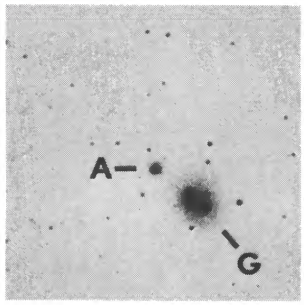

1232.4+1550

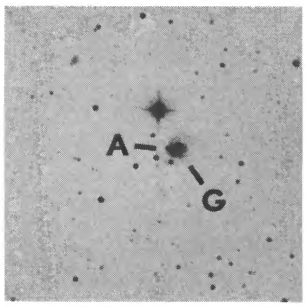

1317.3−1213

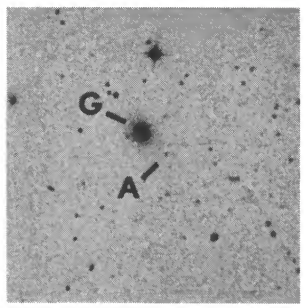

1333.7+0334

FIG. 1.—Finding charts for the X-ray–selected AGNs near galaxies which have not been previously published. In each of these charts the X-ray centroid is at the center of the chart, and the scale and orientation are as given for the first chart. The X-ray–selected AGN is marked with an A and the foreground galaxy with a G. The BL Lac object near NGC 4510 is shown in the first chart marked with an A. Finders for 1E 0038.8−0159, 1E 0104.2+3153, and 1E 1218.7+7522 can be found in Gioia *et al.* (1984) and for 1E 1640.1+3940, in Margon, Downes, and Chanan (1985).

STOCKE *et al.* (*see* page L13)